ORAL/POSTER REFERENCE: ICF10788OR

HIGH-SPEED DEBONDING AND FRICTIONAL SLIDING IN COMPOSITE SYSTEMS: EXPERIMENTAL OBSERVATIONS AND NUMERICAL SIMULATIONS

J. Lambros, X. Bi and P. H. Geubelle

Department of Aeronautical & Astronautical Engineering,
University of Illinois, Urbana, IL 61801

ABSTRACT

This paper reports our recent progress on the experimental and numerical study of dynamic debonding and frictional push-out in model composite systems. A modified Split Hopkinson Pressure Bar system is adopted to perform the dynamic fiber push-out test. A Cohesive Volumetric Finite Element scheme is developed to capture the initiation and propagation of the crack along the fiber/matrix interface. Interface properties are extracted by comparison of experimental and numerical results. Details of the physical process are scrutinized by investigating numerically the propagation and evolution of axial stress along the entire system.

KEYWORDS

Dynamic, residual, debonding, frictional, push-out, SHPB, CVFE

INTRODUCTION

When a crack propagates in a composite material in a direction perpendicular to that of the reinforcing fibers, the failure process involves four basic mechanisms: matrix cracking, fiber/matrix debonding, fiber breakage and fiber pull-out. Under high-velocity impact conditions, a substantial part of the energy is dissipated in the frictional debonding and sliding of the bridging fibers located behind the advancing crack front. Because of the important effect they have on the fracture toughness of a composite, these two processes have been the subject of extensive experimental, numerical and analytical work. Most experimental investigations of fiber debonding and push-out process use model composites, in which a single embedded fiber is pulled or pushed out of the surrounding

matrix. The fiber diameter is typically chosen one to three orders of magnitude larger than that of the actual composite reinforcement to allow for a better control and visual analysis of the failure process. However, the vast majority of existing studies on these topics has been limited to the quasi-static loading case [1,2,3]. The few experimental investigations involving dynamic loading recently performed on various composite systems seem to indicate that the dynamic fiber sliding process presents some unusual and sometimes even contradictory characteristics [4,5]. Recently, existing models has been extended to high loading rates by taking into account the inertial effect of fiber and matrix [6].

The primary objective of this paper is to enhance, through a combined experimental and numerical investigation, the current understanding of *dynamic* debonding and frictional push-out in model fiber-reinforced composites.

EXPERIMENTAL ANALYSIS

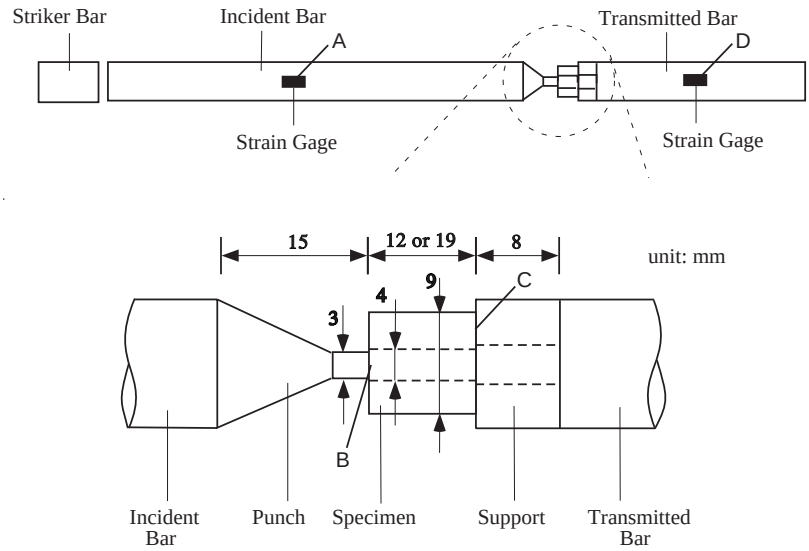

Figure 1: Schematic of the modified SHPB for dynamic fiber push-out test and its connection with a model composite specimen.

To investigate the fiber/matrix debonding and frictional push-out mechanism under high loading rates, a novel experimental setup has been developed and model mono-filament composites have been tested. The high-rate experiments are performed using a modified Split Hopkinson Pressure Bar (SHPB) system (Figure 1). A set of specially designed punch and support connect the model composite with the incident and transmitted bars of the SHPB, respectively. The tapered punch is used to apply compressive loading to a single fiber embedded in a surrounding matrix material. Once the interface debonds, the fiber slides into the hollow support. The contacting ends of the incident bar, punch, composite specimen, support and transmitted bar are connected with each other by grease to allow for free expansion in the radial direction. A schematic of the experimental setup is shown in Figure 1. In this experimental system, the incident bar, punch and support are all made of steel. As the transmitted signal is relatively small, aluminum is chosen for the transmitted bar. The model composite specimen is made in a specially designed mold and cured under room temperature. It consists of a metal fiber (steel or aluminum) embedded in an Epoxy (EPON 862) matrix. Specimen dimensions are also shown in Figure 1. For later use, the dynamic material properties of each individual constituent have been measured using standard high strain

rate SHPB dynamic compression tests. Following the traditional derivation of the SHPB equations, corresponding data reduction equations for the push-out test can be obtained.

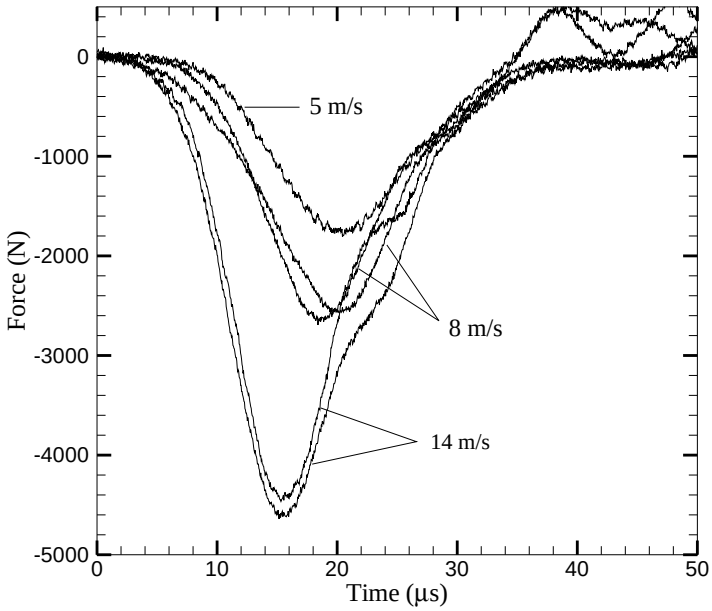

Figure 2: Experimental results: Effect of sliding speed on transmitted force in a model Steel/Epoxy composite (length = 36 mm, grit 36 roughness).

Figure 2 shows the effect of the sliding speed on the transmitted force. We can see from theses curves that both the peak force achieved and the rise time of the signal increase with increasing rate. The figure also illustrates the repeatability of these experiments. Using this technique we have studied the effect of impact speed, material mismatch, fiber length, surface roughness, and residual strain. For more results, please refer to [7].

NUMERICAL ANALYSIS

To process and support these experimental results, a special axisymmetric numerical analysis scheme has been developed and implemented. To extract adequately the complex failure process taking place in the dynamic fiber push-out event, the numerical scheme used in this analysis must account the presence of residual strains in the matrix, the spontaneous motion of the interface debonding front and the frictional contact between the fiber and matrix surfaces. The main component of the numerical method is the cohesive volumetric finite element scheme described hereafter. We then present a summary of the comparison between experimental and numerical results.

Cohesive Volumetric Finite Element Scheme

The spontaneous initiation and propagation of the debonding crack has been captured by a special method referred to as the Cohesive Volumetric Finite Element (CVFE) scheme [8,9]. In our fiber push-out CVFE model, a series of cohesive elements are introduced along the fiber/matrix interface within a conventional finite element mesh as shown in Figure 3. These cohesive elements basically act like nonlinear distributed springs linking standard volumetric elements at interfaces

where failure is possible. The nonlinear springs resist opening (or shearing in this case) in accordance to a prescribed traction-separation law as shown. Eventually, as the separation increases, the cohesive tractions go to zero, simulating the creation of a new free surface. In the general case, the traction-separation law relates the cohesive traction vector, defined by its normal and tangential components, to the displacement jump vector. Figure 3 also shows the relation between the cohesive traction and displacement jump for the pure shear failure. The maximum traction τ_{max} and fracture toughness G_{IIC} characterize the bonding strength of the interface. One goal of this work is to extract these properties by comparing experimental results with numerical analysis. Let us note that this CVFE model was successfully used in the simulation of quasi-static fiber push-out by Lin *et al.* [8].

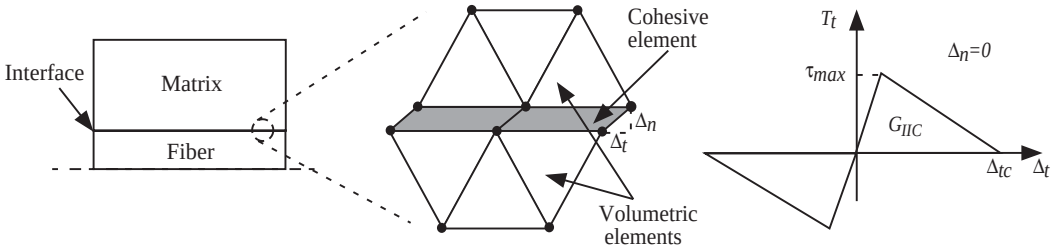

Figure 3: Schematic of interfacial cohesive elements. The two cohesive elements in the center figure are shown in their deformed configuration: in their undeformed configuration, these elements have no thickness and the adjacent nodes are superposed. The quasi-linear cohesive model is shown in the right figure for the pure shear mode.

Comparison between Numerical and Experimental Results

The numerical simulation described hereafter is carried out for an aluminum/EPON specimen, with the stress signal measured from the incident bar in experiments as the load boundary condition. The residual strain in the epoxy matrix is taken as -0.0022 [2]. The material properties of the constituents measured from traditional dynamic SHPB experiments are listed in Table 1.

Table 1: Material Properties of Constituents.

Material Properties	Steel	Aluminum	Epon
E (GPa)	207.0	69.0	5.65
ν	0.30	0.35	0.34
ρ (Kg/m^3)	8130.6	2650.0	1176.0

By fitting the numerical model with experimental results for the 6 m/s impacting speed case, it was found that the interface is characterized by a shear failure strength $\tau_{max} = 60$ MPa, a mode II fracture toughness $G_{IIC} = 150$ N/m, and a friction coefficient $\mu_f = 0.2$. As shown in Figure 4, these interface properties also capture the increase of the peak load with increasing impact speed. Also, the slope of the transmitted stress is well matched with experiments. As indicated by the increasing difference between experimental and numerical peak values of the transmitted stress with increasing sliding speed, these interface properties appear to have small rate sensitivity. For details of the numerical scheme and more simulation results, please refer to [10].

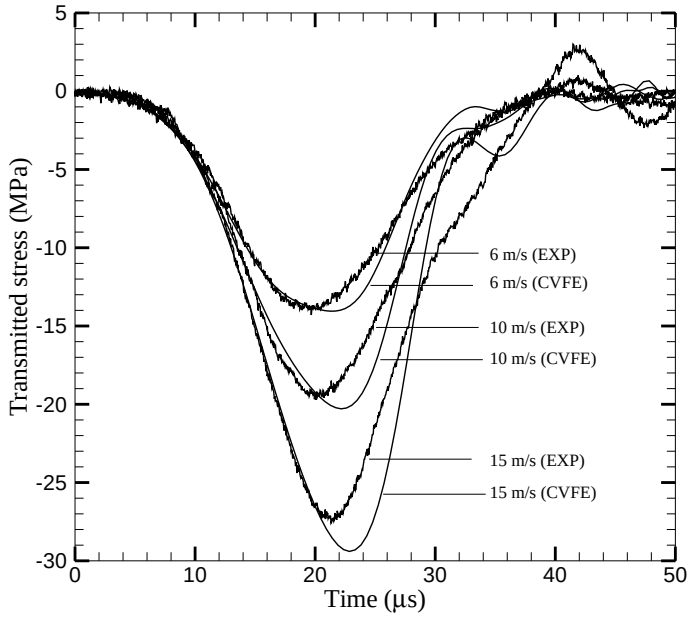

Figure 4: Comparison between numerical and experimental values of the transmitted stress for the model Aluminum/Epoxy composite. All CVFE curves have been computed with $\tau_{max} = 60\ MPa$, $G_{IIC} = 150\ N/m$ and $\mu_f = 0.2$.

Determination of Crack Initiation Point and Propagation Speed

Beyond the comparison with experimental measurement of the transmitted force, the numerical scheme also provides a unique tool to shed more light on the failure process, through a detailed study of the evolution of the axial stress at various locations in the SHPB system. Several observation points (indicated by A, B, C and D in Figure 1) have been tested. The evolution of the axial stress σ_{zz} at three of these points (A, C, D) and that of the crack tip location are presented in Figure 5 for Aluminum/Epoxy composite case (impact speed = 10 m/s) shown in Figure 4. Using the wave speed in the bar, the curve denoting the stress evolution in the middle of the incident bar (point A) is shifted backward in time to match that observed at the interface between the punch and the fiber (point B). To determine the crack initiation time, we performed another elastodynamic simulation in the absence of failure (i.e., by imposing a very high strength τ_{max} in the cohesive model). The corresponding axial stress evolution computed at point C is shown as a dotted curve in Figure 5. At time $t = 18\ \mu s$, we note a clear separation between the point C stress evolution curves with and without failure, indicating the onset of the interface failure process. This crack initiation time is confirmed by the crack tip evolution curve (solid curve in Figure 5). It should be noted that the appearance of the failure-induced kink in the stress curve at point C is unfortunately smoothed out by the time the signal reaches the mid point of the transmitted bar (point D), indicating the need to measure the stress wave closer to the composite specimen [10].
It is interesting to note that, in this particular case, the interfacial crack initiated from the support end of the composite specimen instead of the punch end, as it has been observed for quasi-static experiments involving composite constituents with a high modulus mismatch [2]. Let us note that this behavior also depends on the interface strength: for weak interface, the crack typically starts from the punch end. As indicated in Figure 5, the crack propagates rapidly toward the punch end at a speed of about 1650 m/s, slightly higher than the shear wave speed of epoxy ($C_{se} = 1340\ m/s$) but less than that of Aluminum ($C_{sa} = 3110\ m/s$), i.e., at a speed which is referred to as inter-sonic

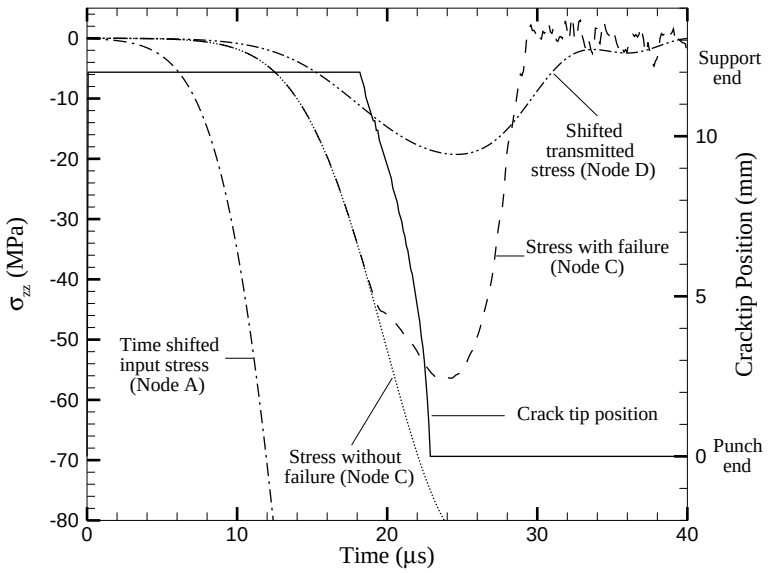

Figure 5: Numerical simulation of the force transfer process for model Aluminum/Epoxy composite with sliding speed of 10 m/s: time evolution of the axial stress at various locations of the push-out setup and of the crack tip location. Time $t = 0$ μs corresponds to the arrival of the initial loading wave at the punch location.

[11]. As the crack length reaches 75% of the fiber length, the crack propagation speed increases further to approximately 5500 m/s which represent 85% of dilatation wave speed in aluminum fiber ($C_d = 6460$ m/s).

ACKNOWLEDGEMENTS

The authors wish to thank the National Science Foundation for the support of this work through grant CMS-9712291.

REFERENCES

1. Tsai, K.-H. and Kim, K.-S. (1996). *J. Mech. Phys. Solids.* 44 (7), 1147.
2. Bechel, V. T. and Sottos, N. R. (1998) *J. Mech. Phys. Solids.* 46 (9), 1675.
3. Liang, C. and Hutchinson, J. W. (1993) *Mech. Mat.* 14, 207.
4. Khanna, S. K. and Shukla, A. (1994) *Exper. Mech.* 171.
5. Klopp, R. W. and Crocker, J. E. (1994) *J. Physique III.* 4, C8.47.
6. Cox, B.N., Sridhar, N. and Beyerlein, I. (2000) Submitted to *J. Mech. Phys. Solids.*
7. Li, Z., Bi, X., Lambros, J. and Geubelle, P. H. (2001) Submitted to *Exper. Mech.*
8. Lin, G., Geubelle, P. H. and Sottos, N. R. (1998) To appear in *Int. J. Solids Structures.*
9. Geubelle, P. H. and Baylor, J. (1998) *Composites (B).* 29B, 589.
10. Bi, X., Li, Z., Geubelle, P.H. and Lambros, J. (2001) Submitted to *Mech. Mat.*
11. Lambros, J. and Rosakis A.J., *J. Mech. Phys. Solids.* 43 (2), 169.